Rapid Communications in Mass Spectrometry

WILEY

Rapid Communications in Mass Spectrometry

RESEARCH ARTICLE

Comparative Metabolomic Analysis of Benzyl Adenine and Meta-Topolin Riboside Treatments in "Tainung No. 1" Passion Fruit

Ying-Chun Chen[1] | Han-Ju Chien[2,3] | Yi-Feng Zheng[4] | Huey-Ling Lin[5] | Chien-Chen Lai[4,6,7,8,9]

[1]Department of Biology, National Museum of Natural Science, Taichung, Taiwan | [2]Department of Biochemical Science and Technology, National Chiayi University, Chiayi, Taiwan | [3]The Education and Research Center of Intelligent Technology for Food and Agriculture, National Chiayi University, Chiayi, Taiwan | [4]Institute of Molecular Biology, National Chung Hsing University, Taichung, Taiwan | [5]Department of Horticulture, National Chung-Hsing University, Taichung, Taiwan | [6]Advanced Plant and Food Crop Biotechnology Center, National Chung Hsing University, Taichung, Taiwan | [7]Graduate Institute of Chinese Medical Science, China Medical University, Taichung, Taiwan | [8]Doctoral Program in Translational Medicine, National Chung Hsing University, Taichung, Taiwan | [9]Rong Hsing Translational Medicine Research Center, National Chung Hsing University, Taichung, Taiwan

Correspondence: Huey-Ling Lin (hllin@dragon.nchu.edu.tw) | Chien-Chen Lai (lailai@dragon.nchu.edu.tw)

Received: 12 August 2025 | **Revised:** 15 November 2025 | **Accepted:** 18 November 2025

Keywords: benzyladenine | metabolomics | *meta*-topolin riboside | passion fruit | Tainung No. 1

ABSTRACT

Rationale: *Meta*-topolin riboside (*m*TR) has shown superior effects over benzyladenine (BA) in promoting root and shoot development in passion fruit tissue culture, yet its underlying mechanisms remain unclear. Understanding the metabolic differences between *m*TR and BA treatments can inform optimized propagation strategies for high-quality planting material in this economically important crop.

Methods: Nodal buds of *Passiflora edulis* "Tainung No. 1" were cultured on BA- or *m*TR-supplemented medium, then analyzed using ultra-high-performance liquid chromatography coupled to quadrupole time-of-flight mass spectrometry (UHPLC-QTOF-MS) in SWATH acquisition mode. Metabolite features were extracted, statistically filtered (VIP > 1, FC > 1.5 or < 0.667, $p < 0.05$), identified via multiple databases, and subjected to enrichment and pathway analysis.

Results: SWATH-MS detected 2823 ions in positive and 1637 in negative mode, with 21 significant metabolites identified in each mode. *m*TR treatment upregulated metabolites linked to root development (e.g., 5,10-methylenetetrahydrofolate, daidzin, and hesperidin) and stem elongation (amygdalin), while BA treatment had higher levels of kinetin, gibberellin A4, and lignans. Pathway analysis highlighted folate metabolism as significantly enriched in *m*TR samples.

Conclusions: *m*TR treatment altered phytohormone, flavonoid and phenolic profiles in ways that likely promote rooting, shoot elongation and oxidative stress resilience, explaining its superior growth performance over BA. These insights can guide refined cytokinin use in micropropagation and broader applications in horticultural biotechnology.

Abbreviations: ACN, acetonitrile; BA, benzyladenine; CES, collision energy spread; CUR, curtain gas; DDA, data-dependent acquisition; ESI, electrospray ionization; FC, fold change; GAs, gibberellins; GC–MS, gas chromatography-tandem mass spectrometry; GS1, gas 1; GS2, gas 2; IAA, indole-3-acetic acid; LC–MS/MS, liquid chromatography–tandem mass spectrometry; MS1, full mass scan; *m*TR, meta-topolin riboside; *m*TTHP, meta-topolin tetrahydropyran-2-yl; OPLS-DA, orthogonal partial least squares discriminant analysis; PC, phosphatidylcholine; PCA, principal component analysis; PVDF, polyvinylidene difluoride; SWATH, sequential window acquisition of all theoretical fragment ion spectra; TEM, temperature; UHPLC–MS/MS, ultrahigh performance liquid chromatography tandem mass spectrometry; UPLC/Q-TOF MS, ultrahigh-performance liquid chromatography-quadrupole time-of-flight mass spectrometry; VIP, variable importance for the projection.

Ying-Chun Chen and Han-Ju Chien contributed equally to this work.

1 | Introduction

Cytokinins are a group of plant growth-regulating substances that play essential functions in the micropropagation system. Benzyladenine (BA), one of the aromatic cytokinins, is the most commonly used type and is often combined with other growth regulators, such as auxin and gibberellin, to regulate its morphogenetic pathways [1, 2]. Although BA is widely used in plant tissue culture to stimulate bud proliferation and morphogenesis, its application is often associated with several physiological disorders. These include vitrification, shoot-tip necrosis, premature senescence, inhibited in vitro rooting, low survival rates during acclimatization and increased somaclonal variation in regenerated plants [3]. Such adverse effects have been reported in various species, including *Aloe vera* [4], sugar beet [5], *Barleria greenii* [6], barley [7], magnolias [8], petunias [9] and bananas [10]. Besides, Aremu et al. studied the regulation of auxin-cytokinin interactions on the organogenesis of leaf-derived adventitious buds in Bromeliads and analyzed the metabolites using UHPLC–MS/MS. They found that most of the metabolites of adventitious buds produced by BA treatment are N^9-glucosides [11], which have been proven to be detrimental to the rooting of in vitro seedlings in various crop tissue culture systems, including Asteria [12], *Harpagophytum procumbens* [13], and *Merwilla plumbea* [14]. *Meta*-topolin riboside (*m*TR) is a ribosylated derivative of *meta*-topolin (*m*T), a hydroxylated benzyladenine analog belonging to the class of aromatic cytokinins known as topolins. Topolins are increasingly favored in plant tissue culture due to their superior physiological responses compared to traditional cytokinins like BA. They can effectively replace BA to promote bud proliferation and regeneration, as demonstrated in various species including crane lily [15], turmeric [16], banana [17], *Pelargonium sidoides* [18], avocado [19], cannabis [20], *Eriocephalus africanus* [21], and *Syzygium cumini* [22]. Among topolin derivatives, *mTR* has attracted attention for its enhanced shoot induction ability, reduced incidence of hyperhydricity, and improved rooting and acclimatization [23, 24]. While substituting *meta*-topolin or *meta*-topolin tetrahydropyran-2-yl (*m*TTHP) for BA in the bud-proliferation culture medium of *Amelanchier alnifolia*, the maximum number of roots was induced, and the highest content of endogenous active cytokinin metabolites and a high amount of free state indole-3-acetic acid were qualitatively and quantitatively analyzed by UHPLC–MS/MS [25]. A recent study elucidated *m*TR's metabolism in woody species, such as *Handroanthus guayacan*, *Tabebuia rosea*, and *Tectona grandis*, revealing that N9-glucosylation is a major deactivation pathway, with notable species-specific differences in hydroxyl repositioning and cytokinin conjugation dynamics [26].

Passion fruit is an economically important commercial crop with growing global demand for high-quality planting material. "Tainung No. 1" is the predominant passion fruit (*Passiflora edulis* × *P. edulis* f. *flavicarpa*) cultivar in Taiwan, which is one of the most economically important varieties cultivated across Southeast Asia, as well as Central and South America. This hybrid produces dark purple fruit with yellow, aromatic flesh, high juice content, and moderate acidity, making it suitable for both fresh consumption and juice processing [27]. Although traditionally propagated through grafting, this method often fails to meet the growing demand for healthy and high-quality planting material. In 2020, Chen et al. were the first to apply *m*TR in the "Tainung No. 1" passion fruit tissue culture system, achieving better effects on in vitro seedling growth and rooting than BA [28]. However, the molecular mechanism remains unclear.

Metabolomics generally refers to the study of the composition, dynamics, interactions, and changes in small organic or inorganic molecules, typically less than 1000 Da, under various environmental disturbances in biological systems. In 2016, Farag et al. employed UPLC-MS and NMR to investigate the metabolite profiles of 17 passion fruit leaf samples, aiming to elucidate their chemical composition and pharmacological potential for drug development. A total of 78 metabolites were identified, including 20 types of C-flavonoids, 8 types of O-flavonoids, 21 types of C, O-flavonoids, 2 types of cyanogenic glycosides, 23 types of fatty acid conjugates, and several newly discovered compounds [29]. SWATH (Sequential Window Acquisition of All Theoretical Fragment Ion Spectra), a type of data-independent acquisition mode, was first proposed by the Aebersold team in 2012. It offers better sensitivity and quantification performance than the traditional data-dependent acquisition (DDA) mode, as it can detect all fragment ions of precursor ions, even if the signal is weak [30]. The standard SWATH method uses a fixed isolation window of 25 *m/z* to acquire data. In 2015, an advanced SWATH method was developed using a variable isolation window, which provides improved quantification capabilities [31, 32]. SWATH-MS is not only useful in proteomics but can also be applied to metabolomics studies [33]. Therefore, this study aims to investigate the metabolome of "Tainung No. 1" passion fruit after treatment with BA and *m*TR, using SWATH-MS to gain insights into the metabolic pathways involved in the nodal bud culture system.

2 | Experimental Section

The experimental workflow is illustrated in Scheme 1. Briefly, nodal buds were individually isolated and cultured on either BA- or *m*TR-supplemented medium, then subcultured without a plant growth regulator. The samples were extracted and analyzed using SWATH-MS technology. After data processing and multivariate analysis, significant features were identified using software. Subsequently, the pathways involving these metabolites were analyzed and discussed.

2.1 | Plant Materials

The official cultivar page of "Tainung No. 1" states that the scientific name is *Passiflora edulis* × *P. edulis* f. flavicarpa. It was developed in the 1980s through hybridization between purple and yellow passion fruit. The page also summarizes key traits such as self-compatibility, sugar–acid ratio, and adaptability to cultivation environments (https://kmweb.moa.gov.tw/subject/subject.php?id=40131). The passion fruit variety "Tainung No. 1" was cultivated in the isolated net house of the Horticultural Experiment Station, Department of Horticulture, National Chung Hsing University (Taichung, Taiwan). Nodal buds excised from mature plants were employed as explants for tissue culture. Each nodal bud was individually cultured on induction medium supplemented with either 1 mg·L^{-1} BA or 1 mg·L^{-1} *m*TR for a period of 4 weeks, followed by subculture on PA2L medium without growth

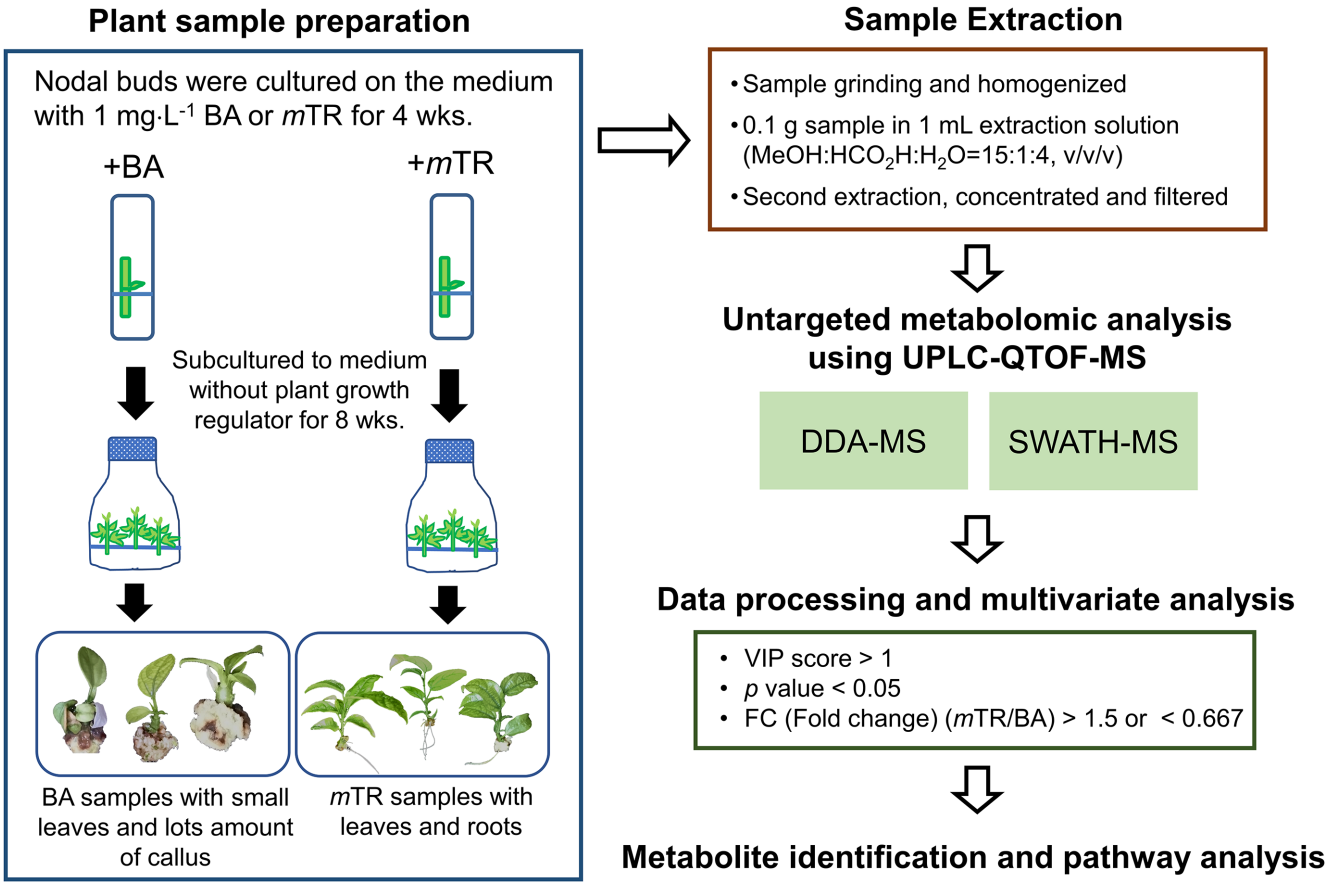

SCHEME 1 | The workflow of this study.

regulators for an additional 8 weeks. The PA2L medium contains MS [34], salts and vitamins, 100 mg·L^{-1} *myo*-inositol, 170 mg·L^{-1} NaH_2PO_4, 20 g·L^{-1} sucrose, 1 g·L^{-1} peptone, 1 g·L^{-1} activated charcoal, 150 mL·L^{-1} coconut water (KOH, BABI Corp International, Thailand), and 6 g·L^{-1} potato powder (PhytoTechnology Labs, USA) and was solidified using 0.86% agar. The pH was adjusted to 5.2 before autoclaving [28]. The entire in vitro plant sample, including callus tissue, was removed, washed, and gently wiped with a paper towel to absorb the water. The samples were then weighed. The appearance of the sampled materials is shown in Figure 1. Each treatment consisted of three samples.

2.2 | Sample Preparation

The extraction procedure was modified from the previous study [35]. The three samples of the same treatment were pooled and placed in a 7-mL homogenizer containing ceramic beads and ground using a Precellys evolution homogenizer (Bertin Technologies, France) at 6800 rpm for 10 s before being cooled on ice for 60 s. This step was repeated once. Next, 0.1 g of the ground sample was weighed into a 2-mL centrifuge tube. The sample was mixed with 1 mL of extraction solvent (methanol: formic acid: deionized water = 15:1:4, v/v/v), vortexed evenly, and left to stand overnight at −20°C. Afterward, the samples were centrifuged at 13 000 g for 20 min at 4°C. The supernatant was transferred to a new Eppendorf tube, and 0.5 mL of the extraction solution was added for a secondary extraction, standing for 1 h at −20°C. The supernatant was then filtered through a 0.22-μm polyvinylidene difluoride (PVDF) filter, dried, concentrated using a SpeedVac at 40°C, and stored at −20°C. Finally, the pellet was resuspended in 30 μL of 50% acetonitrile (ACN) and 120 μL of deionized water and filtered through a 0.22 μm nylon filter before SWATH-MS analysis.

2.3 | Untargeted Metabolomic Analysis Using SWATH-MS

Ultrahigh performance liquid chromatography (UPLC, Ultimate 3000RSLCnano system, Dionex, Thermo Fisher Scientific, Sunnyvale, CA) coupled with a quadrupole time-of-flight mass spectrometer (QTOF-MS, TripleTOF 6600, SCIEX, Framingham, MA) equipped with an electrospray ionization (ESI) source (DuoSpray, SCIEX, Framingham, MA) was used to analyze the metabolite profile. A volume of 5 μL from each sample was injected into a Waters Atlantis T3 C18 column (3 μm, 2.1 × 100 mm). The column temperature was maintained at 35°C, and the flow rate was set at 250 μL min^{-1}. Mobile phase A contained deionized water with 0.1% formic acid, while mobile phase B contained acetonitrile with 0.1% formic acid. The gradient began at 5% B, was maintained for 10 min, increased to 30% B over the next 10 min, reached 90% B over 7 min, and was held for 3 min, then followed by a rapid decrease to 10% B within 0.1 min, which was then maintained for 5 min. The eluted metabolites were then injected into the QTOF-MS for DDA. The MS/MS spectra of precursor ions with a top 20 intensity of more

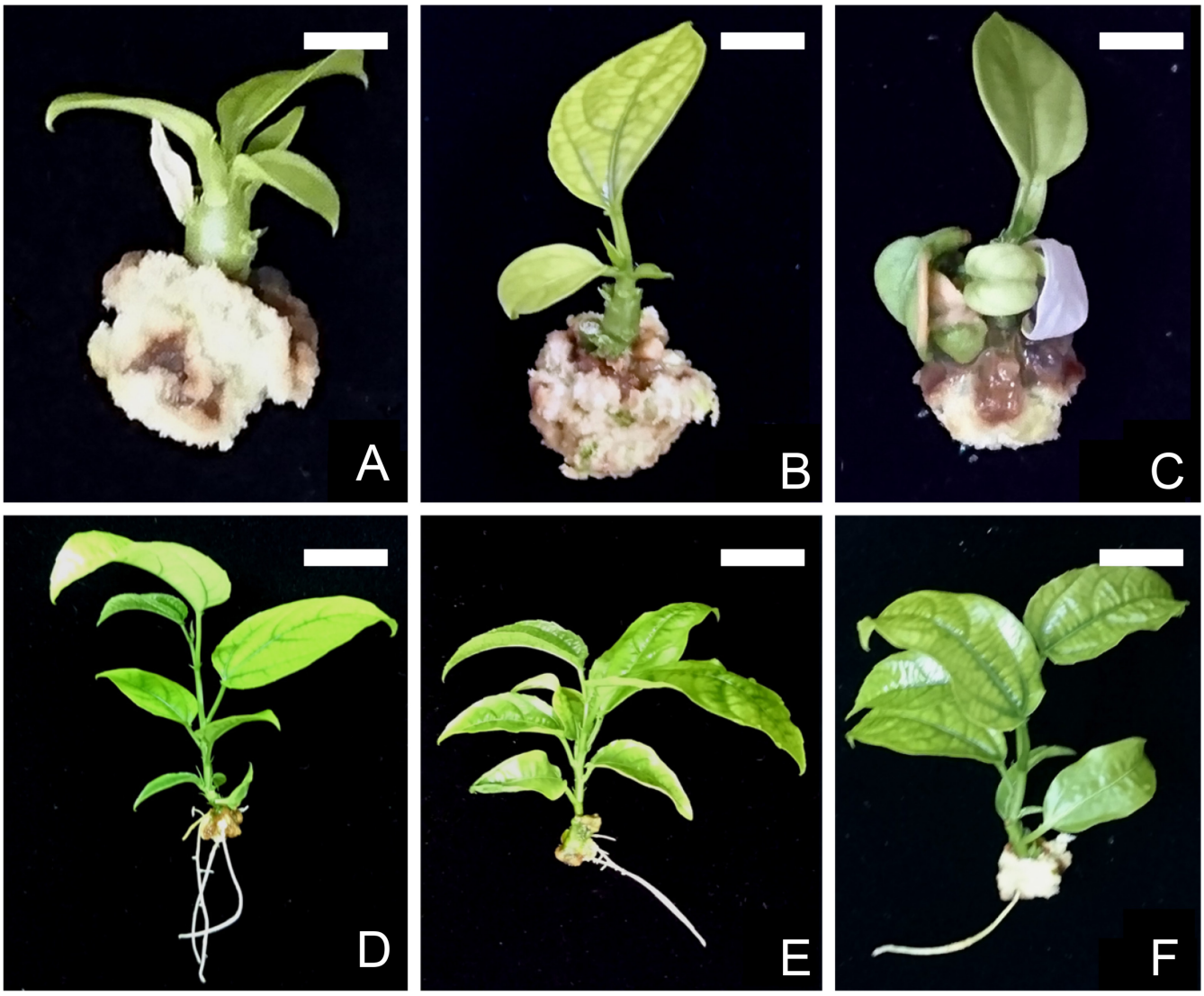

FIGURE 1 | "Tainung No. 1" passion fruit nodal buds were cultured in medium containing 1 mg·L^{-1} BA (a-c) or 1 mg·L^{-1} *m*TR (d-f) for 4 weeks, then subcultured to growth medium for an additional 8 weeks. These materials were used for extraction and analysis. Scale bars: 3.4 mm (a), 6.1 mm (b), 3.6 mm (c), 1.7 cm (d), 1.8 cm (e), 1.1 cm (f).

than 100 cps were acquired using collision-induced dissociation. The mass range for the full mass scan (MS1) was 100 to 1000 *m/z*; for MS/MS, it was 50 to 1000 m/z in positive mode and 100 to 1000 *m/z* in negative mode. The accumulation times for MS and MS/MS were set at 250 and 100 ms, respectively, with an exclusion time of 6 s, including dynamic background subtraction and rolling collision energy. In DDA, extracts from each group, BA and *m*TR treatment groups, were pooled and analyzed in triplicate, serving as the DDA library. SWATH-MS was performed by UPLC-QTOF-MS with accumulation times of 100 ms for MS and 30 ms for MS/MS. The SWATH variable window settings are illustrated in Figure S1 and Table S1, with 40 windows in positive mode and 35 in negative mode, and a collision energy spread (CES) of 15. Each sample in SWATH-MS was analyzed in triplicate. Both DDA and SWATH-MS operated in positive and negative ion modes, applying a voltage of 5500 V for positive ESI (ES+) and −4500 V for negative ESI (ES-). The temperature (TEM) in the ESI source was set at 350°C, with gas 1 (GS1) at 20 psi, gas 2 (GS2) at 15 psi, and curtain gas (CUR) at 25 psi. The ionization gas, curtain gas, and collision gas were nitrogen generated from a nitrogen generator (TJ60–97, Tung Ju Electric Co. Ltd., Japan).

2.4 | Data Processing and Multivariate Analysis

The peak list, which includes retention time, *m/z* value, and peak area in both positive and negative modes from SWATH-MS, was generated using MarkerView v1.3 software (Sciex, Concord, Canada). The parameters for MarkerView are as follows: in peak detection, the noise threshold was set at five counts, the minimum spectra width at ten ppm, and the minimum retention time peak width at three scans; in peak alignment, the retention time tolerance was set at ±0.5 min, and the mass tolerance at 25 ppm; finally, the maximum number of peaks was set at 50000, and the total area sum was chosen as the normalization method.

Principal component analysis (PCA) and orthogonal partial least squares discriminant analysis (OPLS-DA) were executed using SIMCA software (Version 14.0, Umetrics, Sweden). The score

plots and loading plots of PCA and OPLS-DA were analyzed to illustrate the differences between the BA and *m*TR treatment groups. The variable importance for the projection (VIP) score was calculated in OPLS-DA mode. Fold change (FC) and *t*-test analyses were performed using Excel. Before metabolite annotation, significant feature peaks were selected based on the combination of the following criteria: (a) a p-value <0.05, (b) an FC >1.5 or <0.667, and (c) a VIP score >1.

2.5 | Metabolite Annotation and Pathway Analysis

The significant feature peaks were searched using online databases, including the Plant Metabolic Pathway database/PLANTCYC13.0 (PMN; https://plantcyc.org/), ChemSpider (http://www.chemspider.com/), the Kyoto Encyclopedia of Genes and Genomes (KEGG; http://www.genome.jp/kegg/), and PubChem (https://pubchem.ncbi.nlm.nih.gov/). The m/z values of precursor ions were submitted to each database. The mass tolerance was set at ±20 ppm or ± 0.01 Da, and MW or ion types, $[M+H]^+$ or $[M\text{-}H]^-$, were used. For metabolite annotation, PeakView v2.0 software (Sciex, Concord, Canada) was used. The molecular structure used for comparison was obtained from public databases and imported into PeakView software, which automatically generated the predicted fragment list and performed the fragment-matching procedure. Accordingly, the assigned ions were software-generated and not manually selected by the users. The fragment mass error was set at ±0.01 Da. Then, the total intensity of matched peaks (%), the summed intensities of detected fragments in MS/MS spectra, was calculated in each annotation result, which was used as a reference for annotation. In this study, a threshold of 50% matched-peak intensity was applied to retain annotations exhibiting sufficient spectral concordance.

Enrichment analysis and pathway analysis were conducted using MetaboAnalyst 6.0 (https://www.metaboanalyst.ca/MetaboAnalyst/). In the enrichment analysis, a super-class of chemical structures was selected as the metabolite set library. The pathway analysis parameters were as follows: Fisher's exact test was used for the enrichment method, relative-betweenness centrality was used for topology analysis, and *Triticum aestivum* was chosen as the pathway library.

3 | Results

3.1 | Appearance of Buds in BA and mTR Treatments

In our previous research, buds of "Tainung No. 1" passion fruit cultured on medium supplemented with *m*TR could form complete plants with elongated stems and healthy roots. In contrast, buds treated with BA remained in a rosette shape, the base was enlarged, and a large amount of callus was produced. Culturing with these two cytokinins resulted in very different morphological manifestations [28]. The appearance of the buds of "Tainung No. 1" passion fruit used in this study is shown in Figure 1. After 4 weeks of culture in medium containing either BA or *m*TR, most of the buds in the BA treatment were rosette-shaped with delayed growth, and few stems and leaves could elongate (Figure 1A–C). In contrast, the buds in the *m*TR treatment exhibited steady growth, with larger leaves, more stem nodes, and better root development (Figure 1D–F).

3.2 | Metabolite Profiles in BA and mTR Treatments of Passion Fruit

In this study, the possible metabolic pathways were explored using SWATH-MS. The TIC overlays of the samples were shown in Figure S2 and demonstrate good signal stability. A total of 2823 ions were obtained in the positive mode and 1637 in the negative mode. Among these ions, significant feature ions met the criteria of a p-value <0.05, an FC >1.5 or <0.667, and a VIP score >1. In the positive mode, there were 1521 significant feature ions, with 462 ions upregulated and 1075 down-regulated. In the negative mode, a total of 689 feature ions were identified, with 257 ions upregulated and 434 downregulated. The results showed that most differential feature ions were downregulated in the *m*TR treatment.

In the results of the multivariate analyses, the BA and *m*TR samples in both positive and negative modes could obviously be separated in the unsupervised PCA model (Figure 2A); the corresponding loading plot is shown in Figure 2B. The values of R^2X (cum) were 0.925 and that of Q2 (cum) was 0.834, indicating that this PCA model was effective. In the OPLS-DA model, the score plot showed that there was indeed a tremendous difference between the two groups (Figure 3A), and the loading plot is illustrated in Figure 3B. The values of R^2X (cum), R^2Y (cum), and

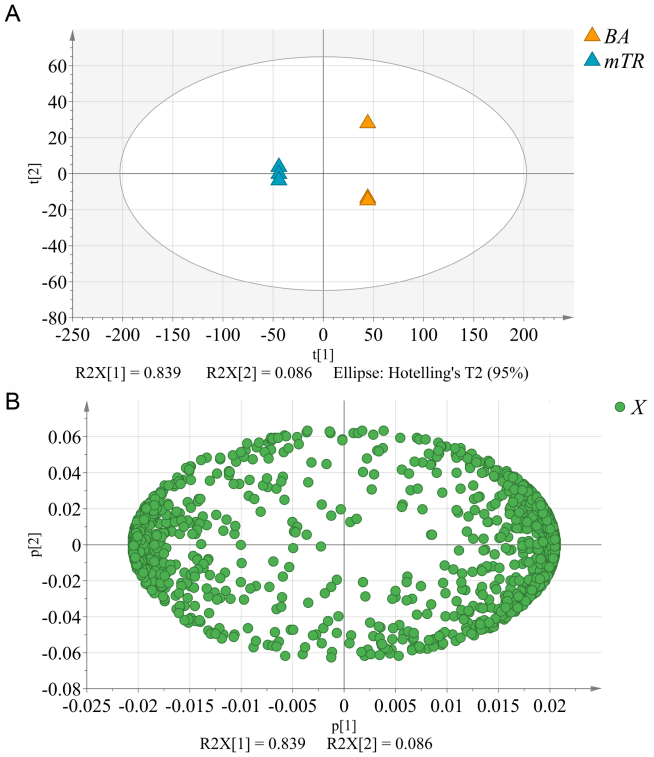

FIGURE 2 | The PCA results for the stem-buds of "Tainung No. 1" passion fruit, which were cultured on medium supplemented with either BA or *m*TR and then subcultured on PA2L medium for 8 weeks, are shown in (A) score plot and (B) loading plot.

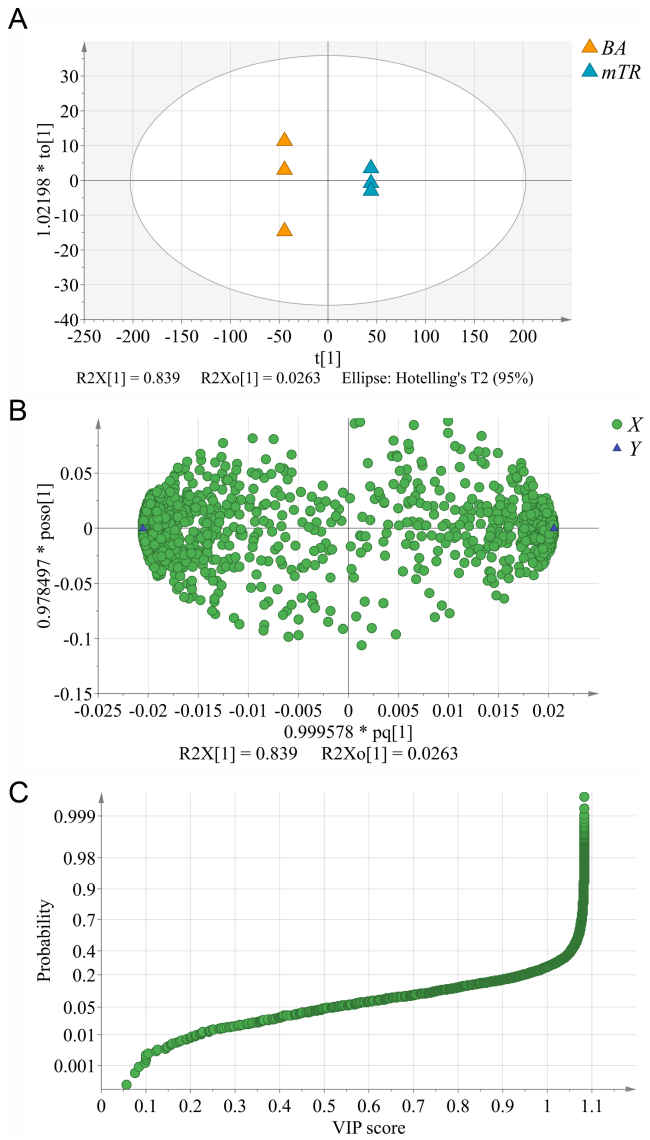

FIGURE 3 | The OPLS-DA results for the stem buds of "Tainung No. 1" passion fruit, which were cultured on medium supplemented with either BA or *m*TR and then subcultured on PA2L medium for 8 weeks. (A) score plot. (B) loading plot. (C) VIP score probability plot.

Q^2 (cum) were 0.865, 1, and 0.999, respectively. The plot of the VIP score is shown in Figure 3C.

In metabolite annotation, 21 metabolites were annotated in positive mode, with 8 upregulated and 13 downregulated (Table 1). In negative mode, 21 compounds were identified, including 3 upregulated and 18 downregulated metabolites (Table 1). The annotation results from the MS/MS spectrum are shown in Figure S3. Subsequently, enrichment and pathway analyses were conducted using MetaboAnalyst. The results of the enrichment analysis classified these significant metabolites into six metabolite sets: (1) phenylpropanoids and polyketides, (2) organoheterocyclic compounds, (3) organic acids and derivatives, (4) lignans, neolignans, and related compounds, (5) organic oxygen compounds, and (6) benzenoids. Among these, lignans, neolignans, and related compounds had the highest enrichment ratio (p-value = 2.1E-2), followed by phenylpropanoids and polyketides (p-value = 4.5E-8) (Figure 4A). Most of these metabolites were from the phenylpropanoids and polyketides and organoheterocyclic compounds (Figure 4B).

3.3 | Pathway Analysis of Differential Metabolites in BA and mTR Treatment

The results of the pathway analysis are illustrated in Figure S4. Only the carbon pool by folate pathway, part of tetrahydrofolate biosynthesis, had a p-value less than 0.05 (p-value = 3.91E-2). The metabolite involved was 5,10-methylenetetrahydropteroyl mono-L-glutamate, also known as 5,10-methylenetetrahydrofolate (5,10-Methylene-THF), and it was 1.93-fold upregulated in *m*TR samples. In a previous study, the folate derivative 5-formyl-tetrahydrofolate, upstream of 5,10-Methylene-THF, was reported to support root meristem maintenance (Lasok et al., 2023). Therefore, we speculate that the upregulation of 5,10-Methylene-THF might improve root development in *m*TR samples.

4 | Discussion

4.1 | Association of Metabolites With Root Development

Among these significant metabolites, kinetin and gibberellin A4 were identified as hormonal compounds. The contents in samples treated with *m*TR were lower than those treated with BA, with FCs of 0.64 and 0.47, respectively. Although no additional growth regulators were added in the experiment, coconut water, which was used and added to the medium, contains auxin-IAA, cytokinin-kinetin, ortho-topolin, gibberellins (GAs), abscisic acid (ABA), salicylic acid (SA), and other plant hormones, thus affecting plant growth [36], thus affecting plant growth. Ge et al. (2005) analyzed and determined the existence of two cytokinins in coconut water, including kinetin and kinetin riboside [37]. Kinetin promotes leaf development and delays senescence. However, high cytokinin content is not conducive to rooting, and the addition of kinetin can inhibit the induction of adventitious roots in *Eucalyptus* [38]. GA-like phytohormones inhibit the formation of adventitious root primordia by controlling the induction and activation mechanisms in Arabidopsis adventitious roots. However, appropriate concentrations of GA can promote the elongation of roots with root primordia [39]. The transformation of root tip growth from cell division to cell expansion can be regulated by histone deacetylase, which inhibits the transcriptional expression of the GA-inactivator gene GA2ox2. Genetic analysis also showed that upregulation of GA2ox2 expression in hdt1 and hdt2 led to a decrease in GA concentration, turning root meristems into transiently enlarged cells [40, 41]. External application of GA inhibited the polar transport of auxin, preventing the formation of the auxin peak at the base of the hypocotyls in poplar and *Arabidopsis thaliana* and reducing the number of adventitious roots [39, 42, 43]. Therefore, the content of kinetin and gibberellin A4 in the BA sample, which had a large amount of callus accumulated at the base without rooting, was higher than in the *m*TR samples with long hairy roots as intact plants. This indicates that lower concentrations of kinetin and GA are conducive to the formation of adventitious roots. Additionally,

TABLE 1 | The differential metabolites of nodal buds in "Tainung No. 1" passion fruit after being cultured in either BA or *m*TR.

Positive mode								
[M + H]+	RT (min)	Formula	Compound name	Characteristic fragment ions	Total intensity of the matched peaks (%)	Fold change	*p*	VIP score
118.06	5.4	$C_8H_7N_1$	Phenylacetonitrile	91.06	95.0	4.02	9.3×10^{-4}	1.05
141.06	6.1	$C_7H_7O_3$	3,5-dihydroxyanisole	95.05, 123.05	88.2	6.76	4.2×10^{-7}	1.06
340.16	4.0	$C_{20}H_{21}N_1O_4$	Papaverine	109.03	52.4	1.58	3.7×10^{-5}	1.06
343.09	2.9	$C_{15}H_{18}O_9$	1-O-caffeoyl-β-D-glucose	153.04, 211.05	85.2	2.23	3.8×10^{-5}	1.06
417.12	10.1	$C_{21}H_{20}O_9$	Daidzin	283.06, 313.07, 337.07, 363.09, 381.10, 399.11	94.0	3.69	5.3×10^{-4}	1.06
458.19	1.0	$C_{20}H_{21}N_7O_6$	5,10-methylenetetrahydropteroyl mono-L-glutamate	116.07	81.9	1.93	4.5×10^{-4}	1.06
579.18	8.7	$C_{27}H_{30}O_{14}$	Apigenin 7-O-neohesperidoside	283.06, 313.07, 397.08, 415.10, 433.10	95.3	2.63	3.3×10^{-6}	1.06
611.19	9.7	$C_{28}H_{34}O_{15}$	Hesperidin	153.04, 239.04, 257.05, 389.09	97.6	1.67	4.4×10^{-4}	1.06
133.07	8.2	$C_9H_8O_1$	Cinnamaldehyde	79.06, 105.07	100.0	0.42	2.3×10^{-3}	1.05
147.07	2.9	$C_5H_9N_2O_3$	3-(carbamoylamino)-2-methylpropanoate	57.04, 71.05, 85.03, 129.06, 130.05	91.0	0.55	5.6×10^{-4}	1.06
177.06	6.4	$C_9H_8N_2O_2$	Phenylhydantoin	117.04, 149.06	71.8	0.59	4.8×10^{-6}	1.06
181.08	4.5	$C_{10}H_{12}O_3$	Dihydroconiferyl aldehyde	81.04, 135.07	88.1	0.65	3.7×10^{-4}	1.05
216.10	1.5	$C_{10}H_9N_5O$	Kinetin	136.07	65.5	0.64	2.9×10^{-5}	1.05
219.06	5.7	$C_9H_{12}O_4S_1$	2-[2′-methylthio]butyl]maleate	97.03, 109.03, 127.04, 173.05, 201.04	100.0	0.54	5.2×10^{-6}	1.06
245.08	1.6	$C_8H_{12}N_4O_5$	5-azacytidine	70.03, 113.04, 133.05	92.9	0.60	3.8×10^{-3}	1.03
251.11	6.6	$C_{10}H_{16}O_5S_1$	2-[(5′-methylthio)pentyl]malate	85.03127.04, 173.05, 191.06	94.3	0.49	2.7×10^{-3}	1.05
282.11	2.8	$C_{12}H_{15}N_3O_3S_1$	Albendazole S-oxide	84.05, 130.05	70.3	0.47	1.6×10^{-3}	1.06
292.11	1.5	$C_{11}H_{17}N_2O_5S_1$	γ-L-glutamyl-(S)-allyl-L-cysteine	84.05, 130.05	100.0	0.64	1.3×10^{-3}	1.04
333.16	8.5	$C_{19}H_{23}O_5$	Gibberellin A4	141.06, 259.12, 291.15	72.5	0.47	1.5×10^{-5}	1.06
338.15	1.5	$C_{12}H_{18}N_2O_9$	3-epihydroxymugineate	84.05, 130.05	93.0	0.62	1.0×10^{-4}	1.06

(Continues)

TABLE 1 | (Continued)

Positive mode								
[M + H]+	**RT (min)**	**Formula**	**Compound name**	**Characteristic fragment ions**	**Total intensity of the matched peaks (%)**	**Fold change**	***p***	**VIP score**
380.15	3.3	$C_{16}H_{21}N_5O_6$	N^6-isopentenyladenine-3-glucuronide (iP3GN)	131.05, 162.02, 234.08, 305.12	69.1	0.18	7.1×10^{-3}	1.94
Negative mode								
[M-H]−	RT (min)	Formula	Compound name	Characteristic fragment ions	Total intensity of the matched peaks (%)	Fold Change	*p*	VIP score
283.07	3.2	$C_{16}H_{11}O_5$	Biochanin-A	151.03	93.5	2.50	1.8×10^{-3}	1.10
456.16	1.1	$C_{20}H_{27}N_1O_{11}$	(R)-amygdalin	118.98, 129.02, 265.06, 341.11	79.4	1.79	9.0×10^{-6}	1.14
593.15	8.5	$C_{30}H_{26}O_{13}$	Kaempferol 3-O-(6”-O-p-coumaroyl)-glucoside	121.00, 137.04, 175.04, 285.04, 327.05, 353.07, 575.14	90.5	4.02	2.2×10^{-6}	1.13
175.06	4.5	$C_9H_8N_2O_2$	Phenylhydantoin	59.01, 115.04	96.5	0.18	7.3×10^{-3}	1.11
250.07	7.6	$C_8H_{13}N_2O_5S^1$	γ-L-glutamyl-L-cysteine	88.04, 132.03	89.9	0.42	5.8×10^{-6}	1.14
251.11	4.6	$C_{17}H_{16}O_2$	Cis-hinokiresinol	101.24, 113.02, 161.05	59.4	0.31	5.6×10^{-3}	1.11
293.12	5.4	$C_{19}H_{18}O_3$	1-phenyl-7-(3,4-dihydroxyphenyl)-hepta-1,3-dien-5-one	59.01, 101.25, 161.05, 251.11	88.2	0.66	1.6×10^{-2}	1.06
311.10	3.1	$C_{13}H_{17}N_3O_4S_1$	(Z)-1-(L-cysteinyglycin-S-yl)-N-hydroxy-2-phenylethan-1-imine	88.99, 161.05, 237.09	73.4	0.42	1.1×10^{-2}	1.09
325.11	4.6	$C_{13}H_{17}N_4O_6$	6,7-dimethyl-8-(1-D-ribityl)lumazine	89.02, 101.25, 161.05	51.4	0.31	7.8×10^{-3}	1.11
325.12	1.0	$C_{12}H_{22}O_{10}$	Rutinose	127.05, 145.06	96.5	0.42	1.9×10^{-4}	1.13
339.12	1.8	$C_{20}H_{20}O_5$	Sophoraflavanone B	113.03, 147.03, 161.05, 311.14	78.0	0.54	1.0×10^{-3}	1.12
353.10	1.7	$C_{20}H_{17}O_6$	(+)-sesamin	307.11, 325.11	50.9	0.64	1.6×10^{-3}	1.12
353.14	2.9	$C_{21}H_{21}O_5$	Xanthohumol	101.02, 161.05, 207.09	83.7	0.49	1.2×10^{-2}	1.09
355.12	1.4	$C_{20}H_{20}O_6$	Leachianone G	88.99, 119.03, 161.05, 327.13	59.4	0.60	5.3×10^{-4}	1.13
363.09	5.7	$C_{21}H_{16}O6$	Justicidin B	111.05, 225.05, 253.05, 355.10	74.6	0.16	6.8×10^{-3}	1.11
380.15	4.9	C16H23N5O6	Trans-zeatin-7-glucoside	71.01, 146.08, 308.14	97.6	0.55	1.5×10^{-2}	1.08

(Continues)

TABLE 1 | (Continued)

Positive mode							
[M + H]+	RT (min)	Formula	Compound name	Characteristic fragment ions	Total intensity of the matched peaks (%)	Fold change	*p*	VIP score
385.13	3.0	$C_{21}H_{22}O_7$	(-)-5′-demethylyatein	88.99, 161.05, 207.09, 283.11, 311.10	94.8	0.37	2.0×10^{-2}	1.05
385.13	1.8	$C_{17}H_{22}O_{10}$	1-O-sinapoyl-β-D-glucose	119.04, 147.05, 175.04, 207.07, 225.08	95.8	0.52	1.9×10^{-4}	1.13
397.11	6.7	$C_{15}H_{19}N_5O_6S_1$	S-adenosyl-4-methylthio-2-oxohutanoate	75.03, 101.04, 119.01, 145.03, 175.04, 189.02, 295.14	96.2	0.29	5.2×10^{-4}	1.12
399.15	2.9	$C_{22}H_{24}O_7$	(-)-yatein	161.05, 207.09, 353.15	91.8	0.47	1.8×10^{-2}	1.08
474.10	5.0	$C_{13}H_{23}N_4O_{11}P_2$	CDP-N-dimethylethanolamine	120.01, 207.01	79.9	0.17	5.6×10^{-3}	1.12

trans-zeatin-7-glucoside and iP3GN, cytokinin metabolites, were expressed in *m*TR samples at 0.55 and 0.18-fold lower than in BA samples.

Phenolic compounds can be classified into four categories based on the structure and quantity of their core skeletons: simple phenolics, lignin, flavonoids, and tannins. Tannins, a secondary metabolite, are mainly synthesized via the shikimic acid pathway and the malonic acid pathway [44]. Flavonoid compounds are essential components of plant root exudates and interact with hormones to participate in the root phototropic response [44]. Previous studies have confirmed that methyl gallate inhibits the root growth of eucalyptus cuttings, and the conversion between the metabolic pathways of gallic acid, shikimic acid, and other flavonoid precursors is a critical factor in the formation of adventitious roots in eucalyptus [45]. Similarly, ellagic acid and its derivatives, which have a structure similar to methyl gallate, also show a lack of rooting ability in chestnut cuttings [46]. The content and distribution of flavonol compounds in the roots of *Arabidopsis thaliana* affect its root system growth. When exposed to light, the roots accumulate flavonols in the phototropic cells, promoting cell elongation and leading to asymmetric growth towards darkness. High flavonol content enhances auxin signaling, PLETHORA (PLT) gradients, and reduces superoxide radical levels, thereby decreasing cell proliferation. Flavonols that accumulate in the root transition zone can reduce taproot growth and promote the formation of new developmental zones. Quercetin, kaempferol, and their glycosyl derivatives play significant roles in Arabidopsis root growth by inhibiting auxin migration and root growth in the dark [47]. Kaempferol and its derivatives also act as IAA-oxidase inhibitors to maintain the dominance of grape buds [48]. In this study, the significant metabolites identified included a variety of phenolic compounds, with the largest number being flavonoid compounds. These included five upregulated metabolites: daidzin with a 3.69-fold increase, apigenin 7-O-neohesperidoside with a 2.63-fold increase, hesperidin with a 1.67-fold increase, biochanin-A with a 2.50-fold increase, and kaempferol 3 -O-(6”-O-p-coumaroyl)-glucoside with a 4.02-fold increase. Three compounds were downregulated: sophoraflavanone B with a 0.54-fold decrease, xanthohumol with a 0.49-fold decrease, and leachianone G with a 0.60-fold decrease. All these compounds belong to the categories of flavones, flavonols, and isoflavones. Most exhibited higher expression in *m*TR samples than in BA samples, indicating that these flavonoid compounds also play a vital role in the root development of passion fruit.

As for CDP-N-dimethylethanolamine, it showed a 0.17-fold down-regulation in *m*TR samples compared to BA samples. This metabolite is involved in phosphatidylcholine (PC) biosynthesis, suggesting that the synthesis of PC might be decreased in *m*TR samples. A previous study found that PC levels were reduced in both the cotyledon and plumule of mung bean seeds during germination, likely because PC was broken down into raw materials such as fatty acids for new membrane synthesis [49]. In this study, the development of both roots and stems was better in *m*TR samples than in BA samples. Therefore, it is speculated that *m*TR samples of passion fruit might exhibit a more significant decrease in PC during the bud sprout and growth processes compared to BA samples, thereby affecting the expression of CDP-N-dimethylethanolamine.

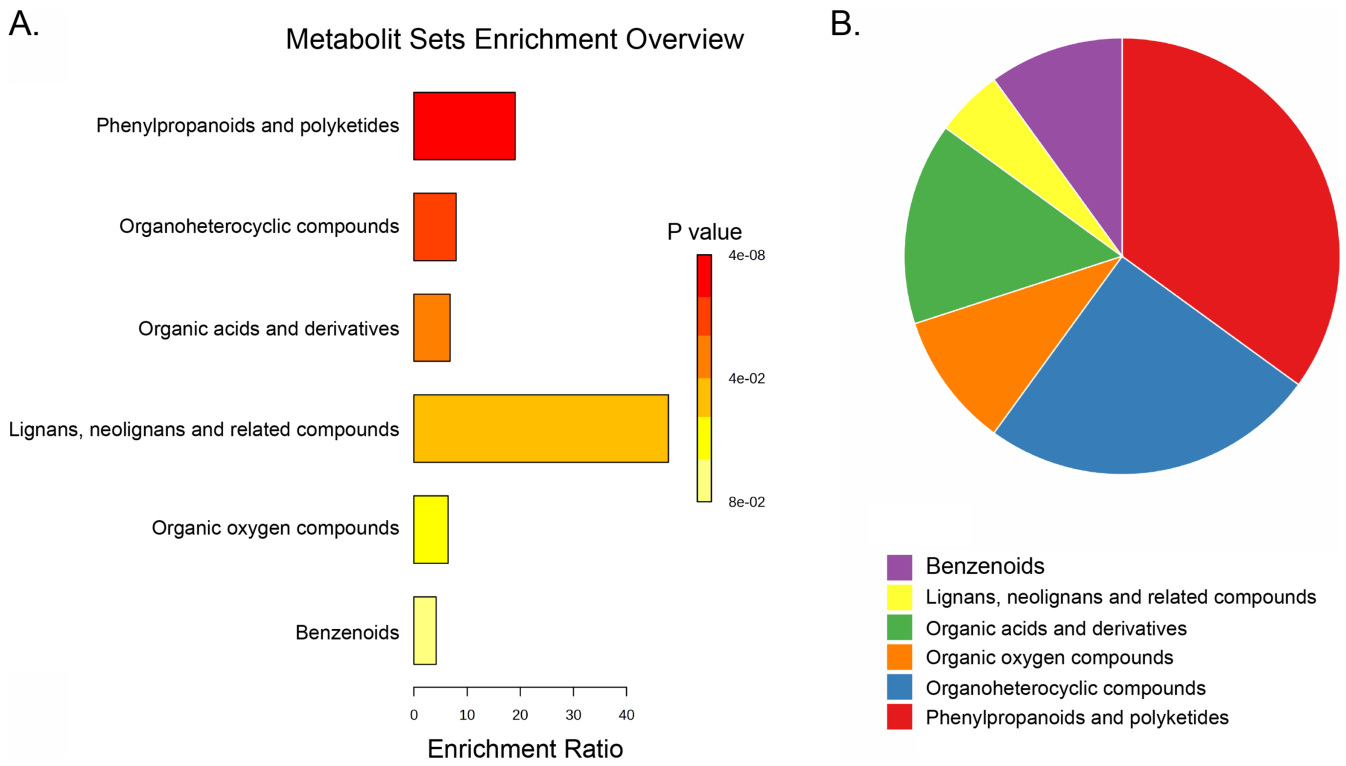

FIGURE 4 | The enrichment analysis results for differentially expressed metabolites include (A) the enrichment ratio plot and (B) the pie chart of metabolite sets classification.

4.2 | Association of Metabolites With Elongated Stems and Leaves

Cyanogenic glycoside is a nontoxic organic compound that can be decomposed by enzymes to form toxic hydrogen cyanide. The types and contents of cyanogenic glycosides in the passion fruit peel and pulp are significantly different. Prunoside is detected only in the peel, where it is the main type of cyanogenic glycoside. The primary and unique cyanogenic glycosides in the pulp are amygdalin and mandelonitrile rhamnosyl β-D-glucopyranoside [50]. Amygdalin is present in the leaves and stems of *Passiflora edulis* and seven other kinds of passion fruit [51]. In this study, the *m*TR samples, which have elongated stems and more leaves, may contain higher levels of cyanogenic glycosides, such as amygdalin, showing a 1.79-fold increase in expression.

4.3 | Association of Metabolites With Plant Defense

Justicidin B, (−)-yatein, (−)-5′-demethylyatein, (+)-sesamin, Nyasol (an cis-hinokiresinol) all belong to lignan compounds, which are often classified as phytoestrogens [52]. The expressions of these compounds in *m*TR samples were significantly lower than those in BA samples, with FCs of 0.16, 0.47, 0.37, 0.64, and 0.31, respectively. Lignans are considered plant defense substances against fungal and viral infections [53]. Meanwhile, 3,5-dihydroxyanisole exhibited a significant 6.76-fold increase in expression in *m*TR samples. This compound belongs to phenolic compounds, which are related to the defense response and possess antibacterial and antifungal activities [54]. A previous study reported that 3,5-dihydroxyanisole is involved in the oxidative stress response, and its expression was higher in Mg deficiency-susceptible grapevine rootstock compared to Mg deficiency-tolerant one. [55]. Here, *m*TR samples had a higher content of 3,5-dihydroxyanisole than BA samples, indicating that *m*TR samples exhibited a greater ability to overcome oxidative stress, potentially resulting in better growth.

4.4 | Guiding Significance of Metabolic Changes for Passion Fruit Cultivation and Quality

In passion fruit tissue culture, explants cultured on BA-supplemented medium frequently exhibited shoot clustering and failed to initiate proper root development, thereby hindering the establishment of a stable tissue culture system. Substitution of BA with *m*TR at an equivalent concentration markedly improved morphogenesis, resulting in well-developed root systems, elongated stems, expanded leaves, and ultimately the regeneration of complete plantlets. These regenerated plantlets were successfully acclimatized, cultivated, and produced fruits [28]. Metabolomic analyses further demonstrated that *m*TR treatment upregulated metabolites associated with root development, such as 5,10-methylene-THF, as well as flavones, flavonols, and isoflavones, while reducing the accumulation of inhibitory compounds, including trans-zeatin-7-glucoside and iP3GN. Moreover, elevated levels of 3,5-dihydroxyanisole were detected, suggesting enhanced antioxidant capacity, which likely contributed to improved growth and vigor.

These metabolic responses indicate that *m*TR, compared to BA, promotes a more favorable hormonal and redox environment for morphogenesis and acclimatization. Therefore,

the metabolomic evidence not only supports the mechanistic basis of improved regeneration but also guides the refinement of culture media formulations. Ultimately, these findings may translate into practical benefits for large-scale propagation, survival rate during transplantation, and possibly the phytochemical quality of passion fruit plants cultivated from tissue culture.

5 | Conclusion

This study is the first to investigate the metabolite profiles of buds cultured on *m*TR or BA medium using SWATH-MS. The appearances of *mT*R samples and BA samples showed significant differences, indicating substantial changes in metabolomes following *m*TR and BA treatments. Several differentially expressed metabolites related to root development, elongated stems, and leaves, and plant defense were identified. Kinetin, gibberellin A4, and some phenolic compounds were found to potentially aid root development, while amygdalin might play a vital role in stem elongation and leaf development. The high expression of these metabolites contributed to the better development of *m*TR samples. Regarding plant defense, although many metabolites decreased in *m*TR samples, 3,5-dihydroxyanisole exhibited much higher expression, with antioxidative ability. Thus, we speculated that this may be one of the reasons for the superior growth observed in *m*TR samples compared to BA samples. Overall, these differences in metabolite expression may contribute to the improved growth of roots and stems in *m*TR-treated passion fruit.

Author Contributions

Ying-Chun Chen: conceptualization, investigation, writing – original draft, visualization, formal analysis. **Han-Ju Chien:** investigation, writing – original draft, methodology, visualization, formal analysis. **Yi-Feng Zheng:** writing – review and editing. **Huey-Ling Lin:** conceptualization, funding acquisition, writing – review and editing, supervision. **Chien-Chen Lai:** conceptualization, funding acquisition, writing – review and editing, supervision.

Acknowledgments

This work was financially (in part) supported by the National Science and Technology Council (NSTC) and the Advanced Plant and Food Crop Biotechnology Center from The Featured Areas Research Center Program within the framework of the Higher Education Sprout Project by the Ministry of Education (MOE) in Taiwan, R.O.C.

Conflicts of Interest

The authors declare no conflicts of interest.

Data Availability Statement

The data that support the findings of this study are available in the Supporting Information of this article.

References

1. M. Ozarowski and B. Thiem, "Progress in Micropropagation of Passifloraspp. to Produce Medicinal Plants: A Mini-Review," *Revista Brasileira de Farmacognosia* 23 (2013): 937–947.

2. D. I. Rocha, C. C. Monte-Bello, and M. C. Dornelas, "Alternative Induction of De Novo Shoot Organogenesis or Somatic Embryogenesis From In Vitro Cultures of Mature Zygotic Embryos of Passion Fruit (*Passiflora edulis* Sims) Is Modulated by the Ratio Between Auxin and Cytokinin in the Medium," *Plant Cell, Tissue and Organ Culture (PCTOC)* 120 (2015): 1087–1098.

3. A. O. Aremu, M. W. Bairu, K. Doležal, J. F. Finnie, and J. Van Staden, "Topolins: A Panacea to Plant Tissue Culture Challenges?," *Plant Cell Tissue and Organ Culture (PCTOC)* 108 (2012): 1–16.

4. M. W. Bairu, W. A. Stirk, K. Dolezal, and J. Van Staden, "Optimizing the Micropropagation Protocol for the Endangered Aloe Polyphylla: Can Meta-Topolin and Its Derivatives Serve as Replacement for Benzyladenine and Zeatin?," *Plant Cell, Tissue and Organ Culture* 90 (2007): 15–23.

5. M. Kubalakova and M. Strnad, "The Effects of Aromatic Cytokinins (Populins) on Micropropagation and Regeneration of Sugar Beet In Vitro," *Biologia Plantarum* 34 (1992): 578–579.

6. S. O. Amoo, J. F. Finnie, and J. Van Staden, "The Role of Meta-Topolins in Alleviating Micropropagation Problems," *Plant Growth Regulation* 63 (2011): 197–206.

7. Z. Huyluoğlu, M. Ünal, and N. Palavan-Ünsal, "Cytological Evidences of the Role of Meta-Topolin and Benzyladenin in Barley Root Tips," (2008).

8. J. K. Parris, D. H. Touchell, T. G. Ranney, and J. Adelberg, "Basal Salt Composition, Cytokinins, and Phenolic Binding Agents Influence In Vitro Growth and Ex Vitro Establishment of Magnolia 'Ann'," *HortScience* 47, no. 11 (2012): 1625–1629.

9. I. Bogaert, S. Van Cauter, S. Werbrouck, and K. Dolezal, "New Aromatic Cytokinins Can Make the Difference," Paper Presented at V International Symposium on In Vitro Culture and Horticultural Breeding, (n.d.).

10. M. W. Bairu, W. A. Stirk, K. Doležal, and J. Van Staden, "The Role of Topolins in Micropropagation and Somaclonal Variation of Banana Cultivars 'Williams' and 'Grand Naine'(Musa spp. AAA)," *Plant Cell, Tissue and Organ Culture* 95 (2008): 373–379.

11. A. O. Aremu, L. Plačková, A. Pěnčík, O. Novák, K. Doležal, and J. Van Staden, "Auxin-Cytokinin Interaction and Variations in Their Metabolic Products in the Regulation of Organogenesis in Two Eucomis Species," *New Biotechnology* 33, no. 6 (2016): 883–890.

12. A. O. Aremu, L. Plackova, J. Gruz, et al., "Accumulation Pattern of Endogenous Cytokinins and Phenolics in Different Organs of 1-Year-Old Cytokinin Pre-Incubated Plants: Implications for Conservation," *Plant Biology (Stuttgart, Germany)* 17, no. 6 (2015): 1146–1155, https://doi.org/10.1111/plb.12367.

13. M. W. Bairu, O. Novák, K. Doležal, and J. Van Staden, "Changes in Endogenous Cytokinin Profiles in Micropropagated Harpagophytum Procumbens in Relation to Shoot-Tip Necrosis and Cytokinin Treatments," *Plant Growth Regulation* 63 (2011): 105–114.

14. A. O. Aremu, L. Plačková, M. W. Bairu, et al., "How Does Exogenously Applied Cytokinin Type Affect Growth and Endogenous Cytokinins in Micropropagated Merwilla Plumbea?," *Plant Cell Tissue and Organ Culture (PCTOC)* 118 (2014): 245–256.

15. S. P. Werbrouck, M. Strnad, H. A. Van Onckelen, and P. C. Debergh, "Meta-Topolin, an Alternative to Benzyladenine in Tissue Culture?," *Physiologia Plantarum* 98, no. 2 (1996): 291–297.

16. N. D. Salvi, L. George, and S. Eapen, "Micropropagation and Field Evaluation of Micropropagated Plants of Turmeric," *Plant Cell, Tissue and Organ Culture* 68 (2002): 143–151.

17. M. W. Bairu, M. G. Kulkarni, R. A. Street, R. B. Mulaudzi, and J. Van Staden, "Studies on Seed Germination, Seedling Growth, and In Vitro Shoot Induction of Aloe Ferox Mill., a Commercially Important Species," *HortScience* 44, no. 3 (2009): 751–756.

18. M. Moyo, J. F. Finnie, and J. Van Staden, "Topolins in Pelargonium Sidoides Micropropagation: Do the New Brooms Really Sweep Cleaner?," *Plant Cell Tissue and Organ Culture (PCTOC)* 110 (2012): 319–327.

19. J. Bandaralage, A. Hayward, C. O'Brien, and N. Mitter, "Gibberellin and Cytokinin in Synergy for a Rapid Nodal Multiplication System of Avocado," Paper Presented at Proceedings of the World Avocado Congress VIII, Lima, (n.d.).

20. H. Lata, S. Chandra, N. Techen, I. A. Khan, and M. A. ElSohly, "In Vitro Mass Propagation of Cannabis Sativa L.: A Protocol Refinement Using Novel Aromatic Cytokinin Meta-Topolin and the Assessment of Eco-Physiological, Biochemical and Genetic Fidelity of Micropropagated Plants," *Journal of Applied Research on Medicinal and Aromatic Plants* 3, no. 1 (2016): 18–26.

21. O. Madzikane-Mlungwana, M. Moyo, A. O. Aremu, et al., "Differential Responses to Isoprenoid, N 6-Substituted Aromatic Cytokinins and Indole-3-Butyric Acid in Direct Plant Regeneration of Eriocephalus Africanus," *Plant Growth Regulation* 82 (2017): 103–110.

22. A. Naaz, S. Hussain, M. Anis, and A. Alatar, "Meta-Topolin Improved Micropropagation in *Syzygium cumini* and Acclimatization to Ex Vitro Conditions," *Biologia Plantarum* 63 (2019): 174–182.

23. N. G. Dimitrova, L. R. Nacheva, D. V. Aleksandrova, M. K. Nesheva, and M. Y. Berova, "Effects of Meta-Topolin Riboside and Meta-Methoxy Topolin Riboside on the In Vitro Micropropagation of *Pyrus communis* L," *Acta Scientiarum Polonorum Hortorum Cultus* 23, no. 5 (2024): 3–15.

24. D. Abdouli, L. Plackova, K. Dolezal, T. Bettaieb, and S. P. O. Werbrouck, "Topolin Cytokinins Enhanced Shoot Proliferation, Reduced Hyperhydricity and Altered Cytokinin Metabolism in *Pistacia vera* L. Seedling Explants," *Plant Science* 322 (2022): 111360, https://doi.org/10.1016/j.plantsci.2022.111360.

25. M. Moyo, A. O. Aremu, L. Plačková, et al., "Deciphering the Growth Pattern and Phytohormonal Content in Saskatoon Berry (Amelanchier Alnifolia) in Response to In Vitro Cytokinin Application," *New Biotechnology* 42 (2018): 85–94.

26. M. Grira, E. Prinsen, and S. Werbrouck, "New Understanding of Meta-Topolin Riboside Metabolism in Micropropagated Woody Plants," *Plants (Basel)* 13, no. 9 (2024): 1281, https://doi.org/10.3390/plants13091281.

27. H.-P. Lo, L.-Y. Lou, and T.-B. Huang, "Establishment of Integrated Propagation System on Grafting Plantlets of Passion Fruit (*Passiflora edulis*)," *HortScience* 58, no. 2 (2023): 170–177.

28. Y.-C. Chen, C. Chang, and H.-L. Lin, "Topolins and Red Light Improve the Micropropagation Efficiency of Passion Fruit (*Passiflora edulis* Sims) 'Tainung No. 1'," *HortScience* 55, no. 8 (2020): 1337–1344.

29. M. A. Farag, A. Otify, A. Porzel, C. G. Michel, A. Elsayed, and L. A. Wessjohann, "Comparative Metabolite Profiling and Fingerprinting of Genus Passiflora Leaves Using a Multiplex Approach of UPLC-MS and NMR Analyzed by Chemometric Tools," *Analytical and Bioanalytical Chemistry* 408, no. 12 (2016): 3125–3143, https://doi.org/10.1007/s00216-016-9376-4.

30. L. C. Gillet, P. Navarro, S. Tate, et al., "Targeted Data Extraction of the MS/MS Spectra Generated by Data-Independent Acquisition: A New Concept for Consistent and Accurate Proteome Analysis," *Molecular & Cellular Proteomics* 11, no. 6 (2012): O111 016717, https://doi.org/10.1074/mcp.O111.01671.

31. Y. Zhang, A. Bilbao, T. Bruderer, et al., "The Use of Variable Q1 Isolation Windows Improves Selectivity in LC-SWATH-MS Acquisition," *Journal of Proteome Research* 14, no. 10 (2015): 4359–4371, https://doi.org/10.1021/acs.jproteome.5b00543.

32. H.-J. Chien, Y.-T. Xue, and C.-C. Lai, "Novel Mass Spectrometry-Based Technique for Quantitative Omics-SWATH," *Chemistry (The Chinese Chemical Society, Taipei)* 74, no. 3 (2016): 235–244.

33. R. Bonner and G. Hopfgartner, "SWATH Data Independent Acquisition Mass Spectrometry for Metabolomics," *TrAC Trends in Analytical Chemistry* 120 (2019): 115278.

34. T. Murashige and F. Skoog, "A Revised Medium for Rapid Growth and Bio Assays With Tobacco Tissue Cultures," *Physiologia Plantarum* 15, no. 3 (1962): 473–497.

35. K. Hoyerova, A. Gaudinova, J. Malbeck, et al., "Efficiency of Different Methods of Extraction and Purification of Cytokinins," *Phytochemistry* 67, no. 11 (2006): 1151–1159, https://doi.org/10.1016/j.phytochem.2006.03.010.

36. J. W. Yong, L. Ge, Y. F. Ng, and S. N. Tan, "The Chemical Composition and Biological Properties of Coconut (*Cocos nucifera* L.) Water," *Molecules* 14, no. 12 (2009): 5144–5164, https://doi.org/10.3390/molecules14125144.

37. L. Ge, J. W. Yong, N. K. Goh, L. S. Chia, S. N. Tan, and E. S. Ong, "Identification of Kinetin and Kinetin Riboside in Coconut (*Cocos nucifera* L.) Water Using a Combined Approach of Liquid Chromatography-Tandem Mass Spectrometry, High Performance Liquid Chromatography and Capillary Electrophoresis," *Journal of Chromatography. B, Analytical Technologies in the Biomedical and Life Sciences* 829, no. 1–2 (2005): 26–34, https://doi.org/10.1016/j.jchromb.2005.09.026.

38. L. R. Corrêa, D. C. Paim, J. Schwambach, and A. G. Fett-Neto, "Carbohydrates as Regulatory Factors on the Rooting of Eucalyptus Saligna Smith and *Eucalyptus globulus* Labill," *Plant Growth Regulation* 45 (2005): 63–73.

39. H. Zhang, C. Dong, F. Li, H. Wang, and Q. Shang, "Progress on the Regulatory Mechanism of Adventitious Rooting," *Acta Botanica Boreali-Occidentalia Sinica* 37, no. 7 (2017): 1457–1464.

40. W. Li, L. Katin-Grazzini, X. Gu, et al., "Transcriptome Analysis Reveals Differential Gene Expression and a Possible Role of Gibberellins in a Shade-Tolerant Mutant of Perennial Ryegrass," *Frontiers in Plant Science* 8 (2017): 868, https://doi.org/10.3389/fpls.2017.00868.

41. K. Shu, W. Zhou, F. Chen, X. Luo, and W. Yang, "Abscisic Acid and Gibberellins Antagonistically Mediate Plant Development and Abiotic Stress Responses," *Frontiers in Plant Science* 9 (2018): 416, https://doi.org/10.3389/fpls.2018.00416.

42. S. Niu, Z. Li, H. Yuan, P. Fang, X. Chen, and W. Li, "Proper Gibberellin Localization in Vascular Tissue Is Required to Regulate Adventitious Root Development in Tobacco," *Journal of Experimental Botany* 64, no. 11 (2013): 3411–3424.

43. M. Mauriat, A. Petterle, C. Bellini, and T. Moritz, "Gibberellins Inhibit Adventitious Rooting in Hybrid Aspen and Arabidopsis by Affecting Auxin Transport," *Plant Journal* 78, no. 3 (2014): 372–384, https://doi.org/10.1111/tpj.12478.

44. T. Tohge, L. P. de Souza, and A. R. Fernie, "Current Understanding of the Pathways of Flavonoid Biosynthesis in Model and Crop Plants," *Journal of Experimental Botany* 68, no. 15 (2017): 4013–4028, https://doi.org/10.1093/jxb/erx177.

45. F. Di Battista, D. Maccario, M. Beruto, et al., "Metabolic Changes Associated to the Unblocking of Adventitious Root Formation in Aged, Rooting-Recalcitrant Cuttings of *Eucalyptus gunnii* Hook. F.(Myrtaceae)," *Plant Growth Regulation* 89 (2019): 73–82.

46. J. Vieitez, D. G. Kingston, A. Ballester, and E. Vieitez, "Identification of Two Compounds Correlated With Lack of Rooting Capacity of Chestnut Cuttings," *Tree Physiology* 3, no. 3 (1987): 247–255, https://doi.org/10.1093/treephys/3.3.247.

47. J. Silva-Navas, M. A. Moreno-Risueno, C. Manzano, et al., "Flavonols Mediate Root Phototropism and Growth Through Regulation of Proliferation-to-Differentiation Transition," *Plant Cell* 28, no. 6 (2016): 1372–1387.

48. P. R. Poudel, I. Kataoka, and R. Mochioka, "Effect of Red- and Blue-Light-Emitting Diodes on Growth and Morphogenesis of Grapes," *Plant Cell, Tissue and Organ Culture* 92 (2008): 147–153.

49. P. Xie, J. Chen, P. Wu, and Z. Cai, "Spatial Lipidomics Reveals Lipid Changes in the Cotyledon and Plumule of Mung Bean Seeds During Germination," *Journal of Agricultural and Food Chemistry* 71, no. 49 (2023): 19879–19887, https://doi.org/10.1021/acs.jafc.3c06029.

50. W. T. Cheng, Q. F. Yuan, T. J. Xiao, et al., "Research Progress on Bioactive Substances and Physiological Functions of Passion Fruit," *Science and Technology of Food Industry* 39, no. 16 (2018): 346–351.

51. R. Gesimba, "The Relationship Between Graft Compatibility and Cyanohydrin Glycoside Type and Content in Passiflora Species," *Annals of Biological Research* 7, no. 8 (2016): 8–12.

52. X. Li, J. P. Yuan, X. Liu, and J. H. Wang, "Lignan: An Important Natural Estrogen From Plants," *Zhongguo Zhong Yao Za Zhi* 31, no. 24 (2006): 2021–2025, https://www.ncbi.nlm.nih.gov/pubmed/17357545.

53. S. Hemmati and H. Seradj, "Justicidin B: A Promising Bioactive Lignan," *Molecules* 21, no. 7 (2016): 820, https://doi.org/10.3390/molecules21070820.

54. D. Lin, M. Xiao, J. Zhao, et al., "An Overview of Plant Phenolic Compounds and Their Importance in Human Nutrition and Management of Type 2 Diabetes," *Molecules* 21, no. 10 (2016): 1374.

55. S. Livigni, L. Lucini, D. Sega, et al., "The Different Tolerance to Magnesium Deficiency of Two Grapevine Rootstocks Relies on the Ability to Cope With Oxidative Stress," *BMC Plant Biology* 19, no. 1 (2019): 148, https://doi.org/10.1186/s12870-019-1726-x.

Supporting Information

Additional supporting information can be found online in the Supporting Information section. **Figure S1:** SWATH variable windows operated in (A) positive and (B) negative modes. **Figure S2:** The TIC overlay of (A) BA and (B) mTR samples in positive and negative mode. **Figure S3:** The identification results from MS/MS spectrum. (A) Phenylacetonitrile; (B) 3,5-dihydroxyanisole; (C) papaverine; (D) 1-O-caffeoyl-β-D-glucose; (E) daidzin; (F) 5,10-methylenetetrahydropteroyl mono-L-glutamate; (G) apigenin 7-O-neohesperidoside; (H) hesperidin; (I) cinnamaldehyde; (J) 3-(carbamoylamino)-2-methylpropanoate; (K) phenylhydantoin; (L) dihydroconiferyl aldehyde; (M) kinetin; (N) 2-[2′-Methylthio]butyl]maleate; (O) 5-azacytidine; (P) 2-[(5′-methylthio)pentyl]malate; (Q) albendazole S-oxide; (R) γ-L-glutamyl-(S)-allyl-L-cysteine; (S) gibberellin A4; (T) 3-epihydroxymugineate; (U) N6-isopentenyladenine-3-glucuronide (iP3GN); (V) biochanin-A; (W) (R)-amygdalin; (X) kaempferol 3-O-(6" -O-p-coumaroyl)-glucoside; (Y) phenylhydantoin; (Z) γ-L-glutamyl-L-cysteine; (AA) cis-hinokiresinol; (AB) 1-phenyl-7-(3,4-dihydroxyphenyl)-hepta-1,3-dien-5-one; (AC) (Z)-1-(L-cysteinyglycin-S-yl)-N-hydroxy-2-phenylethan-1-imine; (AD) 6,7-dimethyl-8-(1-D-ribityl)lumazine; (AE) rutinose; (AF) sophoraflavanone B; (AG) (+)-sesamin; (AH) xanthohumol; (AI) leachianone G; (AJ) justicidin B; (AK) trans-zeatin-7-glucoside; (AL) (−)-5′-demethylyatein; (AM) 1-O-sinapoyl-b-D-glucose; (AN) S-adenosyl-4-methylthio-2-oxohutanoate; (AO) (−)-yatein; (AP) CDP-N-dimethylethanolamine. **Figure S4:** Pathway analysis results of significant metabolites by using metaboanalyst. **Table S1:** SWATH variable windows operated in positive and negative modes.